the plant journal

SEB Society for Experimental Biology

The Plant Journal (2012) **69**, 445–461 doi: 10.1111/j.1365-313X.2011.04804.x

Two AP2 family genes, *SUPERNUMERARY BRACT* (*SNB*) and *OsINDETERMINATE SPIKELET 1* (*OsIDS1*), synergistically control inflorescence architecture and floral meristem establishment in rice

Dong-Yeon Lee and Gynheung An*

Department of Plant Molecular Systems Biotechnology, Crop Biotech Institute, Kyung Hee University, Yongin 446-701, Korea

Received 12 August 2011; accepted 21 September 2011; published online 8 November 2011.
*For correspondence (fax +82 31 204 3178; e-mail genean@khu.ac.kr).

SUMMARY

Meristem identity is crucial in determining the inflorescence architecture of grass species. We previously reported that *SUPERNUMERARY BRACT* (*SNB*) regulates the transition of spikelet meristems into floral meristems in rice (*Oryza sativa*). Here we demonstrated that *SNB* and *Oryza sativa INDETERMINATE SPIKELET 1* (*OsIDS1*) together play important roles in inflorescence architecture and the establishment of floral meristems. In *snb osids1* double mutants, the numbers of branches and spikelets within a panicle are significantly decreased, and the transition to a floral meristem is further delayed compared with the *snb* single mutant. Expression analyses showed that *SNB* and *OsIDS1* are required for spatio-temporal expression of B- and E-function floral organ identity genes in the lodicules. In addition, the AP2 family genes are important for determining the degree of ramification in branch meristems, regulating the spatio-temporal expression of spikelet meristem genes, such as *FRIZZY PANICLE* (*FZP*). Furthermore, overexpression of *microRNA172* (*miR172*) causes reductions in *SNB* and *OsIDS1* transcript levels, and phenotypes of the transgenic plants are more severe than for *snb osids1*. This indicates that additional gene(s) participate in the development of branch and floral meristems. Preferential expression of mature *miR172*s in the area around the spikelet meristems implies that depletion of the AP2 family genes in those meristems via *miR172* is an important step in controlling inflorescence branching and the formation of floral organs.

Keywords: AP2 family, floral meristem, inflorescence, miR172, rice, spikelet.

INTRODUCTION

Grasses have a complex inflorescence architecture, with multiple types of meristems, such as branch and spikelet meristems (Schmidt and Ambrose, 1998; Kellogg, 2007). The inflorescence meristem of rice (*Oryza sativa*) produces several primary-branch meristems until termination. Each then continues to generate next-order meristems laterally until they acquire spikelet meristem identity. Whereas proximal-lateral meristems give rise to secondary branches, distal ones produce spikelet meristems (Ikeda *et al.*, 2004). The key component that determines this architecture is the spatial and temporal regulation of spikelet meristem fate (Kobayashi *et al.*, 2010).

Because the spikelet is the fundamental unit within a grain crop species, elucidating the underlying mechanism for its initiation and growth is crucial for both developmental and agronomic reasons. Several genes that control panicle and spikelet formation have been characterized in rice (Bommert *et al.*, 2005; Bortiri and Hake, 2007). *GRAIN NUMBER1* (*GN1*) and *DENSE AND ERECT PANICLE 1* (*DEP1*) have been identified by quantitative trait locus (QTL) analysis (Ashikari *et al.*, 2005; Huang *et al.*, 2009). *GN1* encodes cytokinin oxidase/dehydrogenase, an enzyme that catalyzes the degradation of cytokinin, implying the involvement of that phytohormone in panicle branching (Ashikari *et al.*, 2005). *DEP1* encodes a protein containing a phosphatidylethanolamine-binding protein-like domain (Huang *et al.*, 2009). *ABERRANT PANICLE ORGANIZATION1* (*APO1*), which encodes an F-box protein related to Arabidopsis *UNUSUAL FLORAL ORGANS* (*UFO*), is a negative regulator of spikelet meristem fate (Ikeda *et al.*, 2007; Ikeda-Kawakatsu *et al.*, 2009). In *apo1*, that fate is determined precociously, leading to the formation of a small panicle. In contrast, enhanced

APO1 expression results in delayed determination of spikelet meristem fate, thus increasing the branch number per panicle. A mutation in *OsMADS34*, a member of the SEPALATA (SEP) family, causes disorganization of panicles and more primary branching (Kobayashi *et al.*, 2010). Plants over-expressing *RICE CENTRORADIALIS1* (*RCN1*) and *RCN2* – homologs of Arabidopsis *TERMINAL FLOWER1* (*TFL1*) – have greater branching and delayed flowering, similar to the consequences of overexpression by *TFL1* (Nakagawa *et al.*, 2002). Rice *FRIZZY PANICLE* (*FZP*), an ortholog of the maize *BRANCHED SILKLESS 1* (*BD1*), regulates spikelet meristem identity (Chuck *et al.*, 2002; Komatsu *et al.*, 2003b). The *fzp* and *bd1* mutants do not establish such identity but, instead, continuously produce branch structures. A mutation of *LAX PANICLE* (*LAX*), encoding a basic helix–loop–helix (bHLH) domain transcription factor, also has fewer branches in its inflorescence (Komatsu *et al.*, 2003a), whereas the RNA interference (RNAi) knockdown of the rice *LEAFY* homolog, *RFL*, has severely diminished panicle branching and increased *FZP* expression (Rao *et al.*, 2008).

Maize *INDETERMINATE SPIKELET 1* (*IDS1*), a member of the AP2 gene family, regulates spikelet-meristem determinacy (Chuck *et al.*, 1998). Spikelets of the *ids1* mutant are indeterminate, producing extra florets. *SISTER OF IDS1* (*SID1*), a paralog in maize, is also crucial for floral meristem initiation and spikelet regulation (Chuck *et al.*, 2008). Because double mutants between *ids1* and *sid1* fail to produce floral organs but generate many bract-like structures, the maize *IDS1* and *SID1* genes appear to function similarly to Arabidopsis *LEAFY* (*LFY*) (Weigel *et al.*, 1992; Chuck *et al.*, 2008). De-repression of these AP2 family genes in *tasselseed4* (*ts4*) and *tasselseed6* (*ts6*) mutants causes extra floret formation and feminization in the tassel spikelet (Chuck *et al.*, 2007). *TS4* encodes *microRNA172* and *ts6* harbors a mutation at the *miR172* target site of *IDS1*. Thus, suppression of *IDS1* and *SID1* expression by *miR172* is crucial in spikelet meristem determinacy. Rice *SUPERNUMERARY BRACT* (*SNB*), an *IDS1*-like gene, is involved in the transition of a spikelet meristem to a floral meristem (Lee *et al.*, 2007). The *snb* mutants display phenotypes of delayed transition and extra bract-like organs.

Despite the successful isolation and characterization of several genes that function in panicle development, our understanding of the molecular basis for rice panicle formation is limited. Here, we studied the roles of two AP2 family genes, *OsIDS1* and *SNB.*

RESULTS

SNB and *OsIDS1* redundantly function in spikelet meristem transition and determinacy

Previously we identified rice mutants defective in *SNB* (Lee *et al.*, 2007). Another AP2 family gene, LOC_Os03g60430, is highly homologous to *SNB* (as per Rice Annotation Release 6.1). Here, phylogenetic analysis showed that *Os03g60430* is closely related to maize *IDS1* (Figure S1b). Therefore, we named it *O. sativa INDETERMINATE SPIKELET 1 (OsIDS1)*. To study its functional roles, we identified an insertion mutant (Line 3A-16852) in the gene from our T-DNA insertion mutant population (Figure S1a in Supporting Information) (Jeon *et al.*, 2000; An *et al.*, 2003; Jeong *et al.*, 2006). Reverse transcriptase-PCR analysis did not detect *OsIDS1* transcripts in the mutant (Figure S1d); thus, the T-DNA insertion generated a null allele.

Spikelets of *osids1* were occasionally abnormal as compared with wild-type (WT) spikelets that consisted of one floret subtending two pairs of glumes – rudimentary glume and empty glume (Figure 1a; Arber, 1934). A normal floret comprises the flower proper (one pistil, six stamens, and two lodicules) plus a pair of bract-like organs (palea and lemma) (Figure 1e; Bommert *et al.*, 2005). In our *osids1* spikelets, one of the empty glumes was occasionally replaced by a rudimentary glume (Figure 1b), and 3.2% of those lodicules were elongated (Figure 1f, Table 1). An extra lodicule also was often found in mutant spikelets (Figure 1f, Table 1).

To examine the functioning of *OsIDS1* further, we generated double mutants between *osids1* and *snb*. Those had more bracts, including rudimentary glumes, lemma, and palea, than did single mutants (Figure 1b–d, Table 1). For example, *osids1* and *snb* plants averaged 4.00 and 4.07 glumes, respectively, versus 4.67 in *snb osids1*. The number of lemma/palea was also increased, to 3.29 in the double mutant from 2.02 and 2.10 in the single mutants. The double mutants rarely developed empty glumes, but elongated bracts were occasionally found in the boundary between a rudimentary glume and lemma. However, their epidermis was similar to that of the lemma/palea (Figures 1d and S2b). Furthermore, ectopic structures were formed between their layers of lemma and palea, sometimes in a reiterated pattern (Figure 1i,j). Scanning electron microscopy (SEM) analyses revealed that these structures contained multiple rudimentary glumes, lemma/palea organs, and rachis (Figure S2c,d), suggesting that they were underdeveloped spikelets. This ectopic structure is similar to that reported with maize *ids1* (Chuck *et al.*, 1998), but differs in that *ids1* has ectopic florets. These observations suggested that *OsIDS1* functions together with *SNB* in spikelet development.

No differences were obvious during the vegetative growth of *snb osids1* double mutants compared with the WT. The former flowered at the same time and showed no apparent differences in plant height or tiller number at maturity. Despite severe reproductive defects, double-mutant panicles occasionally produced a few fertile seeds.

SNB and *OsIDS1* regulate floral organ identity

The *snb osids1* mutants also exhibited abnormal floral organs. Their most conspicuous feature was a change in the

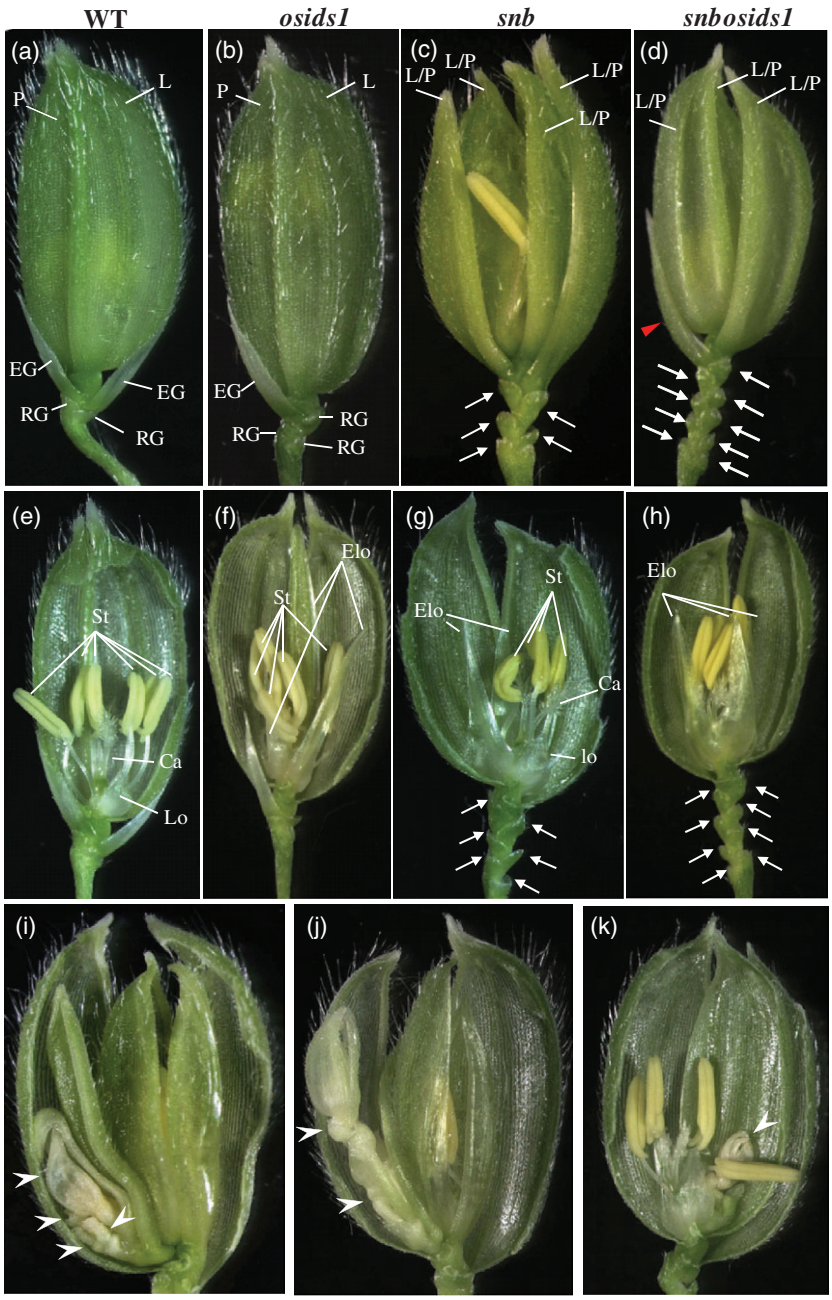

Figure 1. Spikelet phenotypes of *snb*, *osids1*, and *snb osids1*.
(a) Wild-type (WT) spikelet. EG, empty glume; L, lemma; P, palea; RG, rudimentary glume.
(b) *osids1* spikelet.
(c) s*nb* spikelet.
Arrows represent bract-like structure. L/P, lemma/palea-like structure. (d) *snb osids1* spikelet. Red arrowhead indicates intermediate structure between lemma and glume.
(e–h) Upper side of lemma and palea was removed to observe inner floral organs: (e) wild-type spikelet with two lodicules (Lo), six stamens (St), and one carpel (Ca); (f) *osids1* spikelet with three elongated lodicules (Elo); (g) *snb* spikelet with two elongated lodicules, two normal lodicules, four stamens (St), and one carpel (Ca); (h) *snb osids1* spikelet with four elongated lodicules.
(i–k) Spikelets of *snb osids1* double mutants showing ectopic spikelets (arrowheads). Ectopic spikelets were formed between layers of lemma/palea (i, j). Underdeveloped spikelets were formed reiteratively on flank of rachilla. Ectopic spikelet was formed on flank of carpel (k).

size and shape of the lodicules, with approximately 50% being elongated (Figure 1h, Table 1). Moreover, the surface of those elongated lodicules was transformed into those of the lemma and palea (Figure S2c,d). Ectopic lodicules were additionally formed at the side of the palea (Figure 1h), creating a concentric whorl with the original lodicules on the

Table 1 Phenotypic characterizations from different combinations of *snb* and *osids1* alleles

Genotype	Glumes (number)	Lemma/palea (number)	Lodicules (number)	Elongated lodicules (%)	Stamens (number)	Carpels (number)	Spikelets examined (number)
$snb^{+/+}$ $osids1^{+/+}$	4.00 ± 0.06	2.01 ± 0.13	2.00 ± 0.09	0.2	6.00 ± 0.05	1.00 ± 0.00	516
$osids1^{-/+}$	4.00 ± 0.00	2.01 ± 0.09	2.01 ± 0.13	0.5	6.00 ± 0.00	1.00 ± 0.00	215
$snb^{-/+}$	4.00 ± 0.00	2.01 ± 0.12	2.01 ± 0.12	1.4	6.01 ± 0.09	1.00 ± 0.00	140
$snb^{-/+}$ $osids1^{-/+}$	4.00 ± 0.00	2.00 ± 0.13	2.20 ± 0.65	10.7	6.00 ± 0.25	1.00 ± 0.00	300
$osids1^{-/-}$	4.00 ± 0.17	2.02 ± 0.15	2.05 ± 0.24	3.2	6.03 ± 0.32	1.00 ± 0.06	348
$snb^{-/+}$ $osids1^{-/-}$	4.00 ± 0.10	2.56 ± 0.90	2.26 ± 0.65	21.4	5.86 ± 0.48	1.00 ± 0.05	318
$snb^{-/-}$	4.07 ± 0.32	2.10 ± 0.34	2.32 ± 0.69	19.5	5.97 ± 0.41	1.01 ± 0.07	380
$snb^{-/-}$ $osids1^{-/+}$	4.57 ± 1.03	2.52 ± 0.72	2.63 ± 0.86	56.0	5.42 ± 0.97	1.00 ± 0.00	125
$snb^{-/-}$ $osids1^{-/-}$	4.67 ± 0.99	3.29 ± 0.92	2.32 ± 0.96	48.8	4.81 ± 1.27	1.05 ± 0.26	172

Median numbers are shown for each organ. Standard error values are given as ±.

lemma side. These double mutants also had fewer stamens than the WT (Figure 1f–h, Table 1). Although these phenotypes were also observed from the *snb* single mutant (Lee *et al.*, 2007), the double mutants had more severe defects (Table 1). In addition, the double-mutant spikelets generated mosaic organs, e.g. a lodicule–stamen chimera (Figure S3b), a stamen–carpel chimera (Figure S3c), and an indeterminate carpel (Figure S3d), that were not observed from the *snb* mutant.

To study the functional roles for AP2 family genes at the molecular level, we examined their expression in the spikelets and florets. Because most spikelet and floral-organ identities are determined before the panicle reaches 10 mm in length, we collected panicles at two stages: <3 mm and 3–10 mm long. Those shorter panicles largely consisted of spikelets that were about to produce sterile organs such as glumes, whereas the longer panicles contained spikelets in which fertile organs were differentiated.

We first tested the expression of AP1/FUL1 clade genes – *OsMADS14*, *OsMADS15*, and *OsMADS18* – which are mainly expressed in early spikelet meristems and sterile organs (Kyozuka *et al.*, 2000; Pelucchi *et al.*, 2002; Fornara *et al.*, 2004). Quantitative RT-PCR analyses showed that their transcript levels were unchanged in *snb osids1* plants (Figure 2a–c). Hence, delayed floral-meristem transition and floral-organ defects in the mutants appeared to be not associated with AP1/FUL1 clade genes.

We also examined B-function genes, which specify the second and third whorls. Rice has three such genes: *OsMADS2*, *OsMADS4*, and *OsMADS16*. Recessive mutation of *OsMADS16* and suppression of *OsMADS4* results in the transformation of stamens into carpels and lodicules into lemma/palea or bract-like structures (Kang *et al.*, 1998; Nagasawa *et al.*, 2003). Suppression of *OsMADS2*, a *GLOBOSA*-like gene, by RNAi affects development, enlarging the lodicules to palea- or glume-like organs (Prasad and Vijayraghavan, 2003). Here, transcript levels were reduced in young panicles from *snb* or *osids1* single mutants, and even more severely in the *snb osids1* double mutant, especially at the earlier stage (Figure 2d–f). Because expression of B-function genes is restricted in lodicule and stamen primordia (Nagasawa *et al.*, 2003), this decline in transcripts seemed to be caused by delayed development of lodicules and stamens in the mutants. The RNA *in situ* analyses showed that *OsMADS2* transcript in the WT was strongly expressed in the lodicule primordia and weakly in stamen primordia (Figure 3a). In *snb osids1*, that level was decreased, especially in the lodicule primordia, and transcripts disappeared in the region where lodicules had elongated and been transformed into lemma/palea-like organs (Figure 3b).

Transcript levels of the C-function gene *OsMADS3* were also lower in *snb osids1* (Figure 2g). We previously reported that this gene functions in the development of carpels and anthers (Kang *et al.*, 1998). *DROOPING LEAF* (*DL*), a member of the YABBY family, is crucial to assigning carpel identity in the fourth whorl but acts antagonistically with *OsMADS16* (Nagasawa *et al.*, 2003; Yamaguchi *et al.*, 2004). Yamaguchi *et al.* (2004) have reported that *DL* is expressed in carpel primordia and the basal region of the lemma. In *snb osids1*, we detected *DL* expression at the carpel primordia and in the midrib region of the lemma/palea (Figure 3d,e) similar to that observed with the WT (Figure 3c). We also found *DL* expression in the lemma/palea-like organs and elongated lodicules of the mutants (Figure 3e). Although maize *ids1 sid1* spikelets display feminization, i.e. silk formation at the tips of later-developed bracts in ear spikelets (Chuck *et al.*, 2008), we saw no such feminization of the bract-like organs in our rice double mutant (Figure 3). Therefore, it is more plausible that the elongated lodicules acquired lemma identity rather than carpel identity.

Lastly, expression of E-function genes (*OsMADS1*, *OsMADS5*, *OsMADS7*, and *OsMADS8*) was examined. Similar to B- and C-function genes, expression of *OsMADS1* and *OsMADS7* in *snb osids1* was lower than in the WT at the earlier stage (Figure 2h,i). This reduced expression, however, was partially recovered later on (Figure 2). Expression

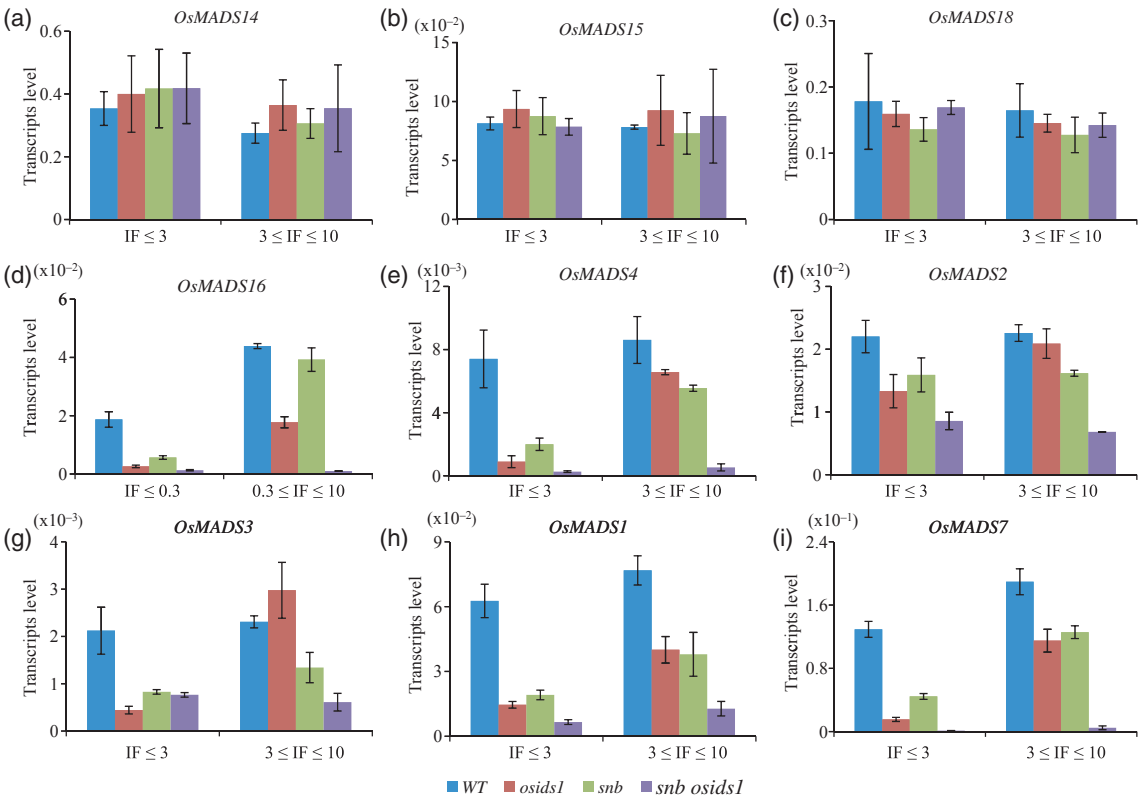

Figure 2. Expression analyses of floral identity genes in wild-type (WT), *osids1*, *snb*, and *snb osids1* mutants.
Quantitative RT-PCR analyses were performed in young inflorescences from each genotype. Bar represents relative values between transcript levels of *ubiquitin1*(*Ubi1*) and regulatory genes: *OsMADS14* (a), *OsMADS15* (b), *OsMADS18* (c), *OsMADS16* (d), *OsMADS4* (e), *OsMADS2* (f), *OsMADS3* (g), *OsMADS1* (h), and *OsMADS7* (i). Two independent experiments were performed for each genotype. Error bars indicate standard deviation. IF ≤ 3, inflorescences shorter than 3 mm; 3 ≤ IF ≤ 10, inflorescences 3–10 mm long.

of *OsMADS5* and *OsMADS8* had patterns similar to that of *OsMADS1* and *OsMADS7* (data not shown). E-function genes are needed for specifying organ identity of the inner three whorls of floral organs in combination with A-, B-, and C-function genes (Pelaz *et al.*, 2000; Honma and Goto, 2001). *OsMADS1* is expressed in the incipient floral primordia but later confined to lemma/palea primordia (Chung *et al.*, 1994; Prasad *et al.*, 2001; Jeon *et al.*, 2008). Our RNA *in situ* experiment had a similar result (Figure 3f). In *snb osids1*, initiation of *OsMADS1* expression was significantly delayed in panicles shorter than 3 mm due to prolonged bract production (Figure 3g). However, this delayed expression was recovered after the floral organ primordia developed (Figure 3i). As stated previously, *OsMADS7* was expressed in the incipient floral meristem immediately after lemma and palea primordia were initiated (Figure 3j). Afterward, this expression was maintained throughout the flower proper, including lodicules, stamens, and carpels, but not in the lemma and palea (Figure 3l) (Greco *et al.*, 1997; Pelucchi *et al.*, 2002). Like *OsMADS1,* initiation of *OsMADS7* expression in *snb osids1* fell behind that of the WT (Figure 3k). As floral organs emerged, that expression was excluded in the elongated lodicules and confined to the inner two whorls in *snb osids1* (Figure 3m). Our RT-PCR and RNA *in situ* analyses showed that the delay in floral meristem initiation in *snb osids1* was substantiated by late and reduced expression of floral organ identity genes. These observations supported our conclusion, at the molecular level, that floral meristem development was delayed and, consequently, floral meristem identities were reduced in *snb osids1*.

Spikelet phenotypes of *snb ids1* are dose- and photoperiod-dependent

Introducing an *osids1* heterozygote (*osids1*$^{-/+}$) into a homozygous *snb* (*snb*$^{-/-}$) background enhanced the mutant phenotypes (Table 1). The number of lemma/palea was increased to 2.52 in *snb*$^{-/-}$ *osids1*$^{-/+}$ from 2.10 in *snb*$^{-/-}$ (Table 1). The number of glumes and frequency of elongated lodicules also rose in *snb*$^{-/-}$ *osids1*$^{-/+}$ as compared with *snb*$^{-/-}$ (Table 1). Likewise, the introduction brought subtle effects on other phenotypes (Table 1). Plants of *snb*$^{-/+}$ *osids1*$^{-/-}$ had more severe phenotypes than did the *osids1* or *snb* single mutants in the lemma/palea and

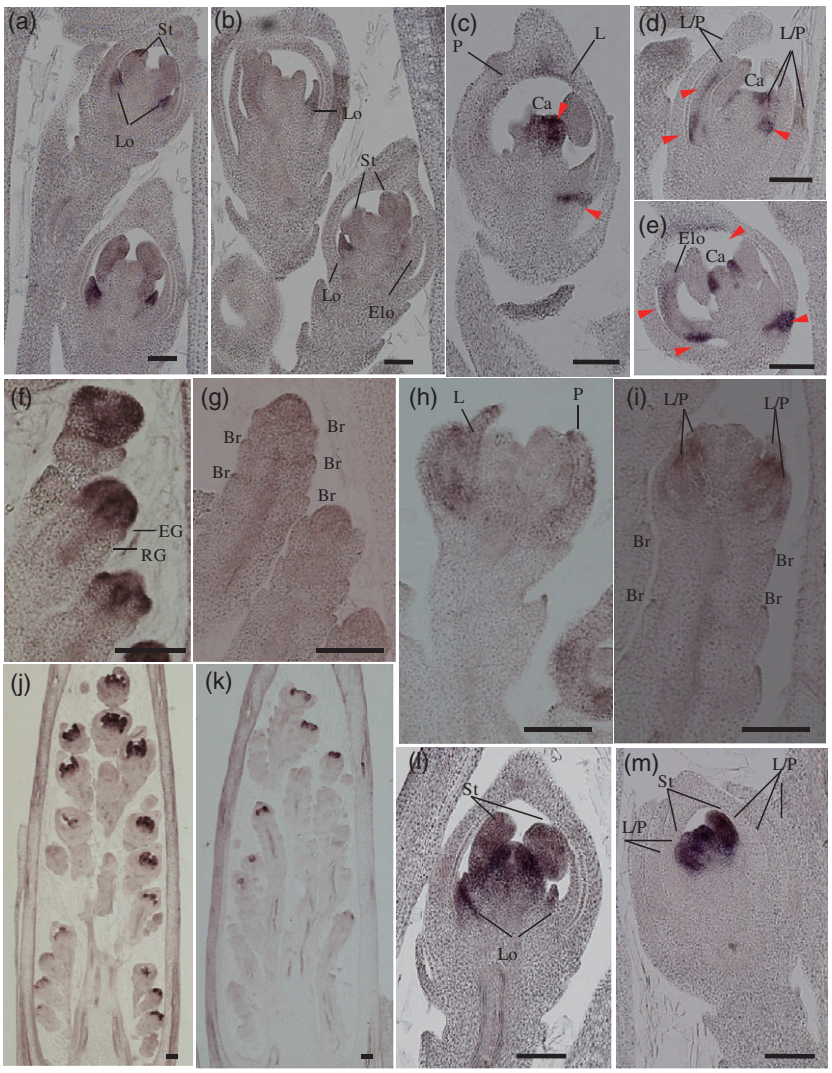

Figure 3. *In situ* hybridization of organ identity genes in wild-type and *snb osids1* mutants.
(a, b) *OsMADS2* expression patterns for wild-type (a) and *snb osids1* (b) at floral meristem stage upon initiation of stamen primordia.
(c–e) *DL* expression patterns for wild-type (c) and *snb osids1* spikelets (d, e) at floral meristem stage upon initiation of carpel primordia. Arrowheads indicate locations of expression.
(f, g) *OsMADS1* expression patterns for wild-type (f) and *snb osids1* (g) at spikelet meristem stage upon initiation of empty glumes and bracts.
(h, i) *OsMADS1* expression patterns for wild-type (h) and *snb osids1* (i) at floral meristem stage upon initiation of palea/lemma primordia.
(j, k) *OsMADS7* expression patterns for wild-type (j) and *snb osids1* (k) in 3-mm-long inflorescences.
(l, m) *OsMADS7* expression patterns for wild-type (h) and *snb osids1* (i) at floral meristem stage upon initiation of stamen primordia.
Wild-type and mutant samples were placed on same slide for hybridization. Br, bract; Ca, carpel; EG, empty glume; Elo, elongated lodicules; L, lemma; Lo; lodicule; L/P, lemma/palea; P, palea; RG, rudimentary glume; St, stamen. Scale bar = 100 μm.

lodicule (Table 1). These observations indicated that *SNB* and *OsIDS1* function semi-dominantly and synergistically contribute to floral meristem fate in a dose-dependent manner.

Dose-dependency in the increment of glumes and lemma/palea was more evident in *snb*$^{-/-}$ *osids1*$^{-/+}$ than in *snb*$^{-/+}$ *osids1*$^{-/-}$ (Table 1). For example, the number of glumes was significantly increased in *snb*$^{-/-}$ *osids1*$^{-/+}$ but not in *snb*$^{-/+}$ *osids1*$^{-/-}$. Lodicules numbered 2.63 in the former and 2.26 in the latter. The reduction in the number of stamens was also more significant in the former. These differences were likely due to the degree of expression, i.e. the *SNB* transcript level in the inflorescences was approximately eight times higher than for *OsIDS1*.

Unexpectedly, we found more lodicules and a higher frequency of lodicule elongation in *snb*$^{-/-}$ *osids1*$^{-/+}$ compared with *snb*$^{-/-}$ *osids1*$^{-/-}$ (Table 1). This might have been due to unambiguous morphology between lemma/palea and elongated lodicules in the double mutant, where the number of lemma/palea was significantly increased.

The mutant phenotypes were more severe under long days (LD) compared with short days (SD), with individual spikelets having more glumes and lemma/palea under LD conditions (Figure S4a,b). Elongated lodicules also occurred more frequently under LD (Figure S4c). Under SD, most spikelets of *snb* were nearly normal in their numbers of glumes and lemma/palea. Because LD are unfavorable for flowering, these enhanced phenotypes were probably due to an extended period of floral induction.

SNB and *OsIDS1* control the duration of inflorescence and branch meristems

In addition to their defects in floral meristem transition, panicles of *snb osids1* produced fewer primary branches and spikelets than the WT (Figure 4a). Wild-type 'Dongjin' panicles averaged 13 nodes, from each of which a branch grew. These primary branches also had several nodes that each produced secondary branches and lateral spikelets. Branches cease to develop terminal spikelets (Hoshikawa, 1989; Itoh *et al.*, 2005). Our *snb* and *osids1* single mutants had fewer branches and spikelets than the WT (Fig 4b,c). In the *snb osids1* double homozygotes, the number of primary branches was further decreased to 8.27 (62%), and the number of spikelets in the mutant was about one-half that of its WT siblings (70 versus 141). These reductions indicated that inflorescence meristems and branch meristems precociously lose the ability to maintain their fate and then terminate or convert to next-order meristems.

To determine whether these defects in panicle architecture are dose dependent, we examined the mutants in different *snb* and *osids1* genotype combinations. The *snb* heterozygote plants produced fewer primary branches and total spikelets than the WT but more than the homozygous mutant (Figure 4b,c). Similarly, *osids1* heterozygous plants had intermediate phenotypes between homozygous plants and the segregating WT (Figure 4b,c). In double-mutant combinations, the degree of phenotype was proportional to the number of *snb* and *osids1* mutant alleles. This positive relationship of primary branches and spikelet counts to the number of active *SNB* and *OsIDS1* alleles demonstrated that both genes regulate the duration of inflorescence and branch meristems in a dose-dependent manner.

SNB and *OsIDS1* positively regulate panicle branching by repressing spikelet meristem identity

We examined expression of *FZP*, which controls spikelet meristem identity. Because a loss of its function results in excess panicle branches without spikelets, *FZP* is apparently necessary for spikelet meristem development (Komatsu *et al.*, 2003b). Quantitative RT-PCR analyses showed that its transcripts were significantly increased in panicles from *snb* single and *snb osids1* double mutants (Figure 5a). This gene is expressed at the semi-circular domain above rudimentary glumes only when the spikelet meristem is forming

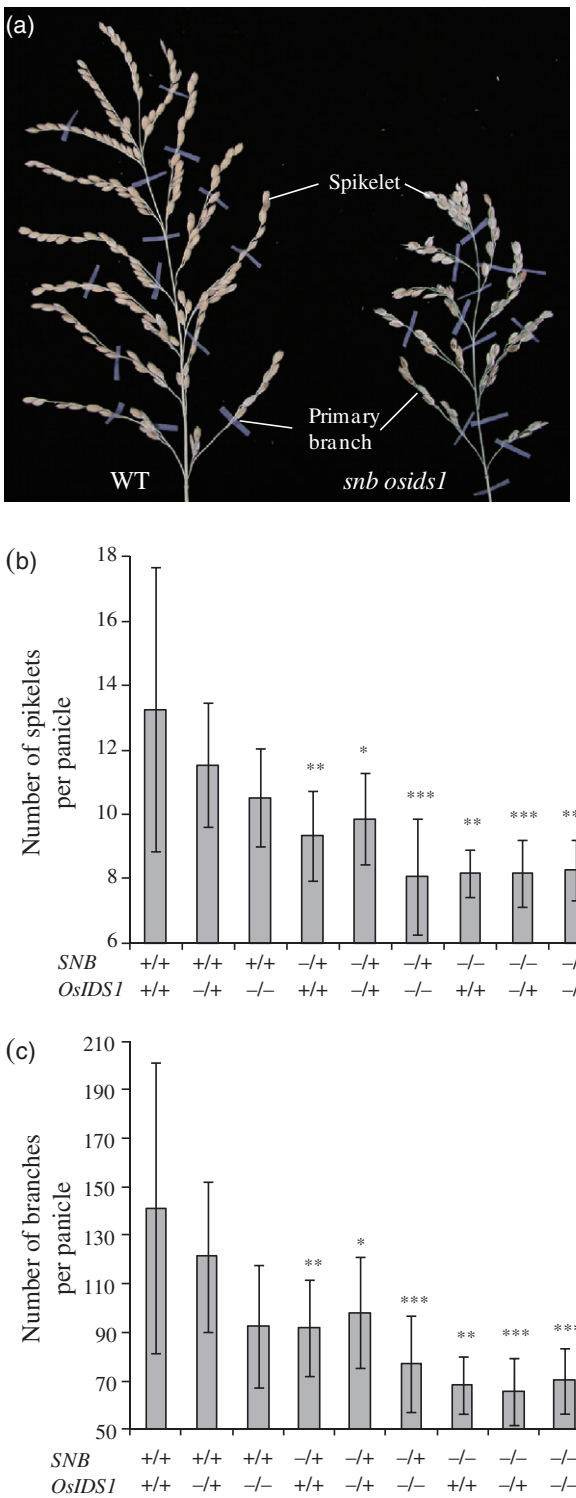

Figure 4. Inflorescence architecture.
(a) Comparison of inflorescence between wild type (WT) and *snb osids1*. (b) Average number of primary branches per panicle.
(c) Average number of spikelets per panicle.
At least 10 panicles from main culms were used for analysis. Asterisks indicate significant differences from wild type at $*P < 0.05$; $**P < 0.01$; or $***P < 0.001$.

(Komatsu *et al.*, 2003b). Our RNA *in situ* experiments confirmed that transcripts were located primarily in the region where rudimentary glumes were appearing in that meristem (Figure 5c). However, transcripts were not detected in the branch meristems before spikelet meristems were determined (Figure 5b). In *snb osids1*, *FZP* transcripts were found earlier in branch meristems and secondary branch meristems (Figure 5d,e). This early expression indicated that branch meristems in *snb osids1* were precociously determined to spikelet meristems. As the *snb osids1* spikelet meristem grew, ectopic expression of *FZP* was detected in the upper region of the bract primordia (Figure 5f,g).

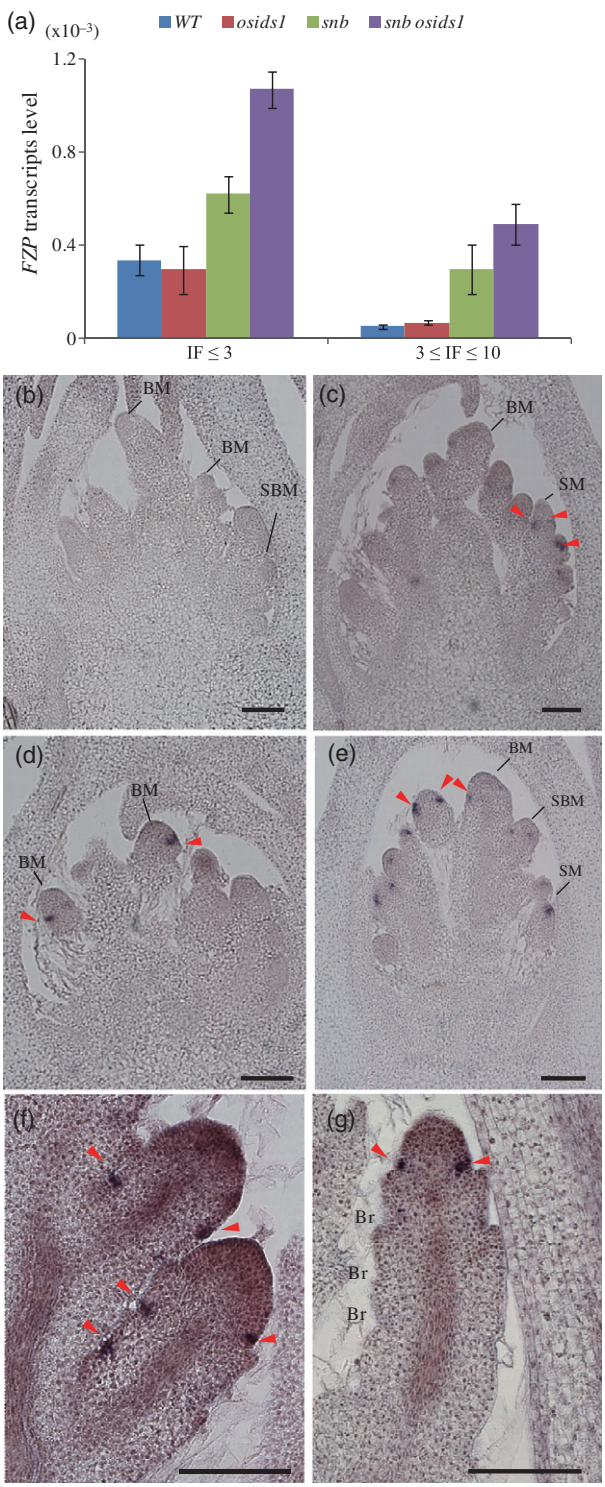

Figure 5. Expression patterns of *FZP*.
(a) Quantitative RT-PCR analyses of *FZP* in young inflorescences. Each data point is the average of two or more independent experiments. Bars represent relative values between transcript levels of *FZP* and *Ubi1*. Error bars indicate standard deviation. IF ≤ 3, inflorescences shorter than 3 mm; 3 ≤ IF ≤ 10, inflorescences 3–10 mm long.
(b, c) *FZP* expression in wild type at branch meristem stage (b) and spikelet meristem initiation stage (c).
(d, e) *FZP* expression in *snb osids*1 at branch meristem stage (d) and spikelet meristem initiation stage (e).
(f, g) *FZP* expression in *snb osids1* at stage bearing bracts continuously.
Arrowheads indicate incidence region of expression.
Scale bar = 100 μm. BM, branch meristem; Br, bract; SBM, secondary branch meristem; SM, spikelet meristem.

Comparison of expression patterns between *OsIDS1* and *SNB*

Previously we reported that *SNB* is more abundantly expressed in incipient branch meristems and spikelet meristems (Lee *et al.*, 2007). Here, we compared its expression patterns with those of *OsIDS1*. Quantitative RT-PCR analyses showed that *SNB* transcripts were highly abundant in seedlings and developing panicles, whereas those of *OsIDS1* were much less abundant at all developmental stages except for seedling shoots, during which time both genes were almost equally expressed (Figure 6a). RNA *in situ* hybridization revealed that *OsIDS1* was detected in developing branch and spikelet meristems at very early stages of inflorescence formation (Figure 6b,c). Expression of *OsIDS1* was maintained uniformly in the spikelet meristems until floral organs were initiated (Figure 6d,f,g). Afterward, transcripts were evenly detected in floral organ primordia (Figure 6h). In contrast, *SNB* transcripts were more abundant in incipient rudimentary- and empty-glume primordia (Figure 6i–k). Although *OsIDS1* was expressed at a lower level than was *SNB*, patterns were similar for both genes during most developmental stages examined. This explains why *osids1* had a weaker but redundant phenotype compared with that of *snb1*.

Expression of *FZP* and *SNB* overlaps in spikelet meristems

The untimely expression of *FZP* in *snb osids1* plants prompted us to examine whether expression of *FZP* and the AP2 family genes overlapped. We performed double RNA *in situ* hybridization using digoxigenin (DIG)-labeled *SNB* and fluorescein-labeled *FZP* probes. *SNB* expression was maintained in the branch and spikelet meristems during inflorescence development (Figure 7a,b). Meanwhile, *FZP*

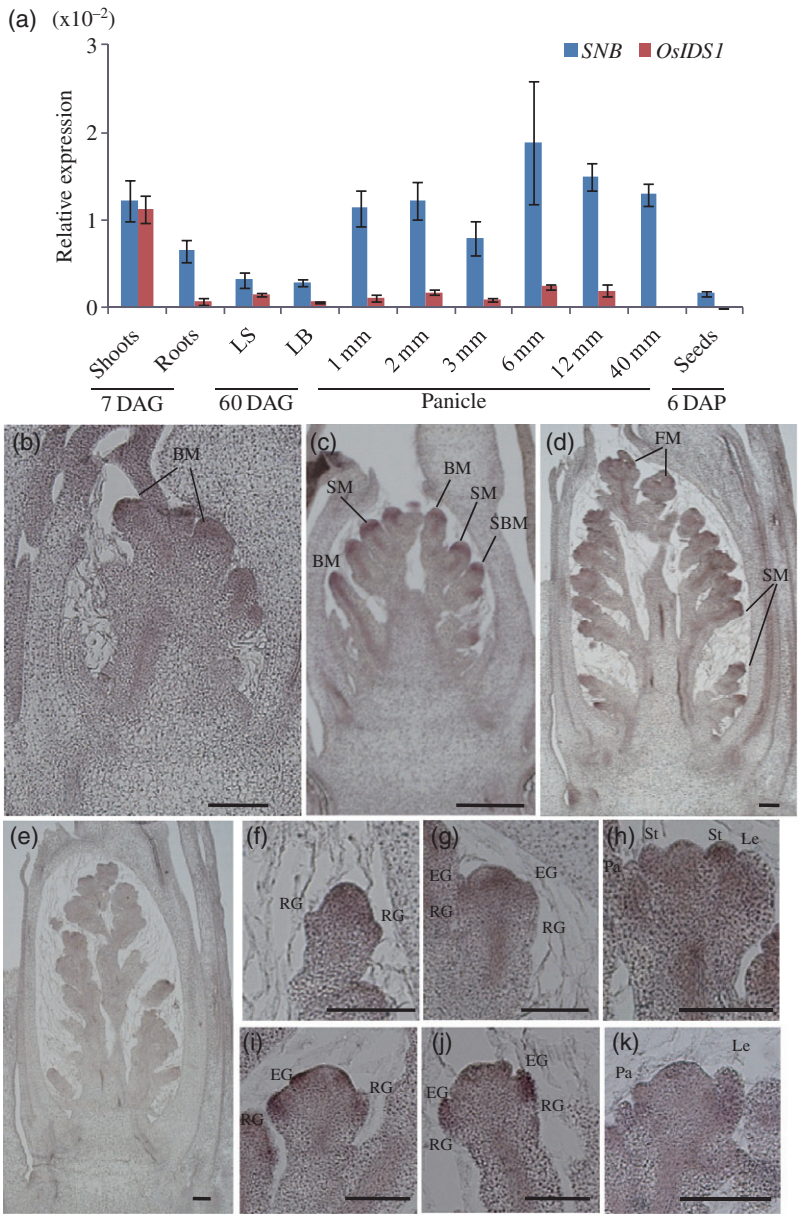

Figure 6. Quantitative RT-PCR and RNA *in situ* hybridization analyses of *SNB* and *OsIDS1*.
(a) Quantitative RT-PCR analysis in various organs. Each bar represents relative values between transcripts levels of regulatory genes and *Ubi1*. Error bars indicate standard deviation. DAG, days after germination; DAP, days after pollination.
(b–d) RNA *in situ* hybridization of *OsIDS1* in wild-type developing panicles at an early stage of branch meristem initiation (b), late stage of branch meristem initiation (c), and spikelet meristem transition stage (d).
(e) *OsIDS1* sense control.
(f–h) *OsIDS1* expression pattern in spikelet meristem.
(i–k) *SNB* expression pattern in spikelet meristem.
BM, branch meristem; SBM, secondary branch meristem; SM, spikelet meristem; FM, floret meristem; RG, rudimentary glume; EG, empty glume; Le, lemma; Pa, palea; St, stamen. Scale bar = 100 μm.

expression was first detected in the abaxial region of branch meristems where the spikelet meristem emerged (Figure 7c). After the spikelet meristems branched off, its expression was located in the half-ring domain where rudimentary glumes were predicted to appear (Figure 7d). These analyses showed that *FZP* and *SNB* expression overlapped partially and temporarily. However, in the later stages, expression of each gene diverged: *FZP* expression was retained in the regions between the rudimentary glume and empty glume, whereas *SNB* expression was shifted to the

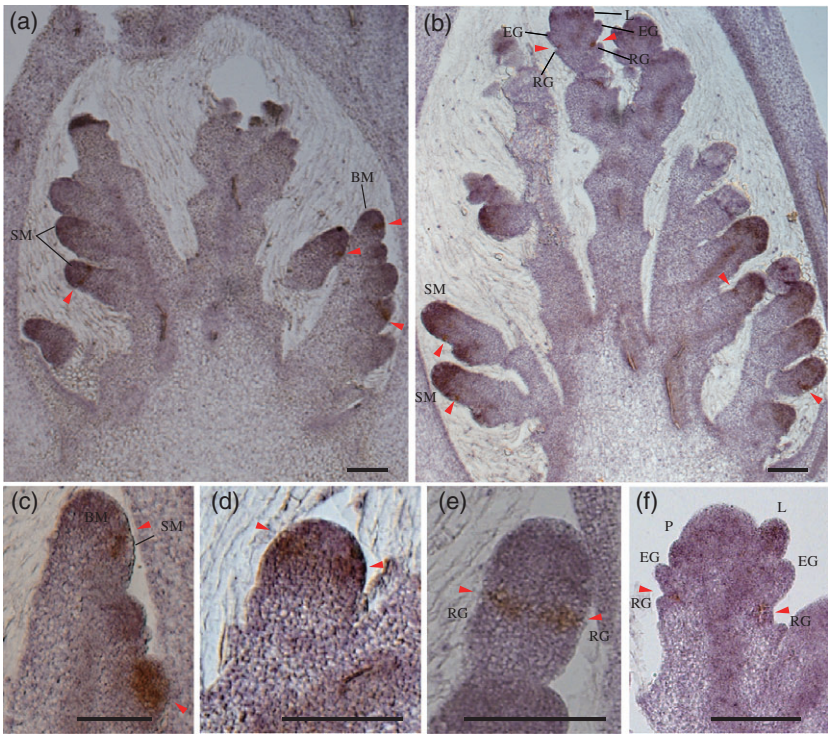

Figure 7. Double RNA *in situ* hybridization of *SNB* and *FZP1*.
(a) Panicle with branch meristems and spikelet meristems.
(b) Panicle in which rudimentary glumes have emerged from most spikelet meristems. At top, spikelet meristems produced lemma primordia.
(c–f) Magnified images of spikelet meristems at stage of spikelet meristem emergence (c), before rudimentary glume primordia emerged (d), after rudimentary glume primordia appeared (e), and at stage of palea/lemma primordia emergence (f).
The digoxigenin (DIG)-labeled *SNB* probe was detected with NBT/BCIP substrate (purple and blue); fluorescein-labeled FZP probe, with INT/BCIP substrate (orange and red). Red arrowheads indicate expression domain of *FZP*. BM, branch meristem; EG, empty glume; Le, lemma; Pa, palea; RG, rudimentary glume; SM, spikelet meristem. Scale bar = 100 μm.

dome region of meristems and anlagen of the glume primordia (Fig 7b,e,f).

Overexpression of *osmiR172* mimics *snb osids1* phenotypes

AP2 family genes are known targets of *miR172* (Aukerman and Sakai, 2003; Schmid *et al.*, 2003; Chen, 2004; Lauter *et al.*, 2005; Chuck *et al.*, 2007). In rice, *miR172*s are encoded by at least four loci that give rise to the same or almost identical microRNAs (Sunkar *et al.*, 2005; Zhu *et al.*, 2009) (Figure 8a). To determine whether *SNB* and *OsIDS1* are targeted, we generated transgenic rice plants with elevated levels of *miR172.* Genomic fragments spanning the fold-back structures of *miR172a*, *-b*, *-c*, and *-d* were placed under the control of the maize *Ubiquitin* (*Ubi*) promoter. Transgenic plants over-expressing these different *miR172*s showed similar phenotypes, albeit with some variation in the severity of their defects (Figure 8c–i). All were somewhat smaller and flowered early (Figure 8c), and their panicle architecture was significantly altered. Their numbers of primary branches and total spikelets were also significantly reduced (Figure 8d), and they developed several bract-like structures at the base of their spikelets (Figure 8f–i). Some plants had panicles with a solitary spikelet at the tip of each branch but no lateral spikelets (Figure 8c, right). In these severe alleles, most spikelets continuously generated bracts and terminated with distorted leaf-like hulls that lacked any floral organs (Figure 8g), while others produced stamens and carpels (Figure 8h,i). Plants with mild phenotypes had fertile floral organs that generated mature seeds.

Transcripts for *miR172* were more abundant in the transgenics compared with their segregating WT siblings; those levels were correlated with the severity of the phenotype (Figure 8b). These phenotypes were similar to those of the *snb osids1* double mutants, but were more severe in the *miR172* plants, implying that another AP2 family gene (in addition to *SNB* and *OsIDS1*) is involved in panicle development. Therefore, these analyses showed that rice *miR172* genes participate in regulating spikelet development and meristem cell fate.

Transcript levels of *SNB*, *OsIDS1*, and *Os06g43220* are regulated by *miR172*

To determine whether *SNB* and *OsIDS1* are regulated by *miR172*, we performed quantitative RT-PCR analyses of young inflorescences from the *miR172*-overexpressing plants (Figure 9). Because the transgenic plants with severe

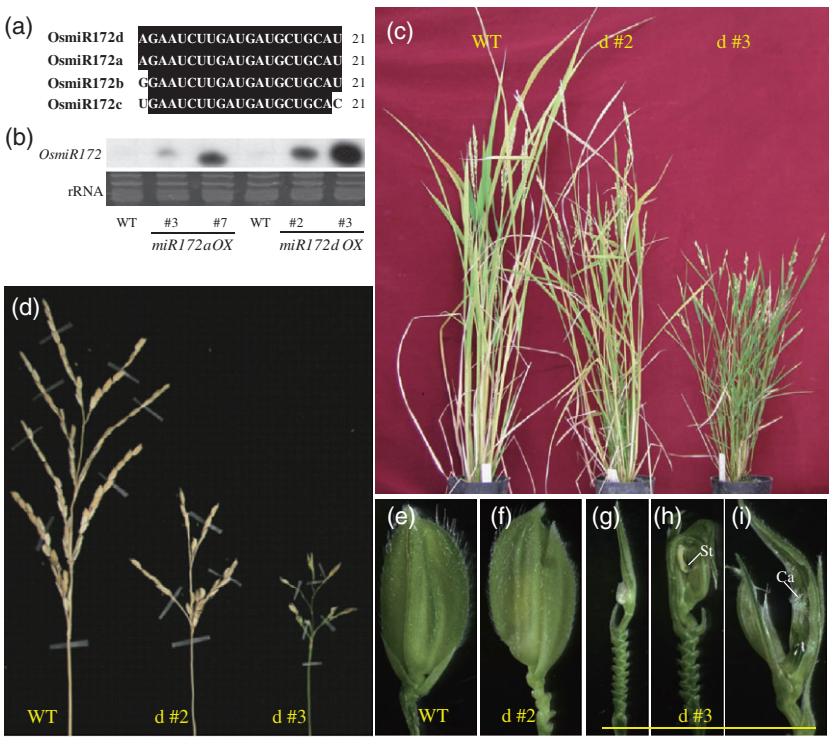

Figure 8. Phenotypes and expression analysis of *OsmiR172*-overexpressing plants.
(a) Sequence comparison of four rice *microRNA172*s.
(b) Comparison of mature *OsmiR172* levels among wild-type (WT) and *miR172*-overexpressing plants. RNAs were prepared from mature flag-leaves for gel blot assay (top). Ethidium bromide-stained ribosomal RNA was used as loading control (bottom).
(c, d) Architecture at harvesting stage (c), and panicle architecture (d).
Plants from left to right are segregant WT from transgenic line no. 2, *Ubq*::*miR172d* no. 2 transgenic plant, and *Ubq*::*miR172d* no. 3 transgenic plant. (e) Spikelet from WT.
(f) Spikelet from *Ubq*::*miR172d* no. 2 showing mild phenotype.
(g–i) Spikelets from *Ubq*::*miR172d* no. 3 with severe phenotypes. St, stamen; Ca, carpel.

phenotypes did not produce fertile seeds, we instead used those with more moderate phenotypes. The mRNA levels of *SNB* and *OsIDS1* were significantly reduced in the transgenics compared with the WT (Figure 9a,b). These results indicated that elevated expression of *miR172* led to a decline in the steady-state levels of *SNB* and *OsIDS1* transcripts.

We also addressed whether other AP2 family genes are affected. Among their five genes that occur in rice, *Os04g55560* appears to be pseudo- or non-functional (Zhu *et al.*, 2009; Figure S1). Therefore, we determined transcript levels for the remaining two genes. Expression of *Os06g43220* was reduced in the transgenic plants, especially in *miR172a* no. 4 (Figure 9c), which showed higher levels of *miR172a* expression compared with the no. 3 plants (Figure 9g). Meanwhile, transcripts for *Os05g03040* were unchanged (Figure 9d). Therefore, these three AP2 genes are probably miR172 targets in inflorescence development.

The phenotype was more severe for transgenic plant no. 4 than for no. 3 (Figure 9e,f). This outcome was correlated with overexpression of the microRNA (Figure 9g) and the reduced level of *Os06g43220*. *SNB* and *OsIDS1* transcripts were not entirely reduced in the overexpressing plants, even in those that displayed more severe phenotypes than from the *snb osids* double mutants (Figure S5). These findings indicated that, in addition to *SNB* and *OsIDS1*, *Os06g43220* plays a role in controlling inflorescence development.

Expression analysis of *miR172* in rice

To examine the expression patterns of *miR172*, we performed stem–loop RT-PCR (Chen *et al.*, 2005; Varkonyi-Gasic *et al.*, 2007). Our objective was to distinguish *miR172b* and *miR172c* from *miR172a* and *miR172d* because they differ by only one base at the 5′ or 3′ ends (Figure 8a). However, control tests with synthetic *miR172* oligonucleotides could not discriminate among these *miR172*s (data not shown). Therefore, we were able to measure only the total mature *miR172* levels. These experiments demonstrated that total *miR172*s were abundant in the leaf sheaths of 30-day-old plants and in the inflorescence meristems during the early developmental stages (Figure 10a). For confirmation, we conducted RNA gel-blot analyses with a locked nucleic acid (LNA) antisense to the *miR172* (Kumar *et al.*, 1998). Similar

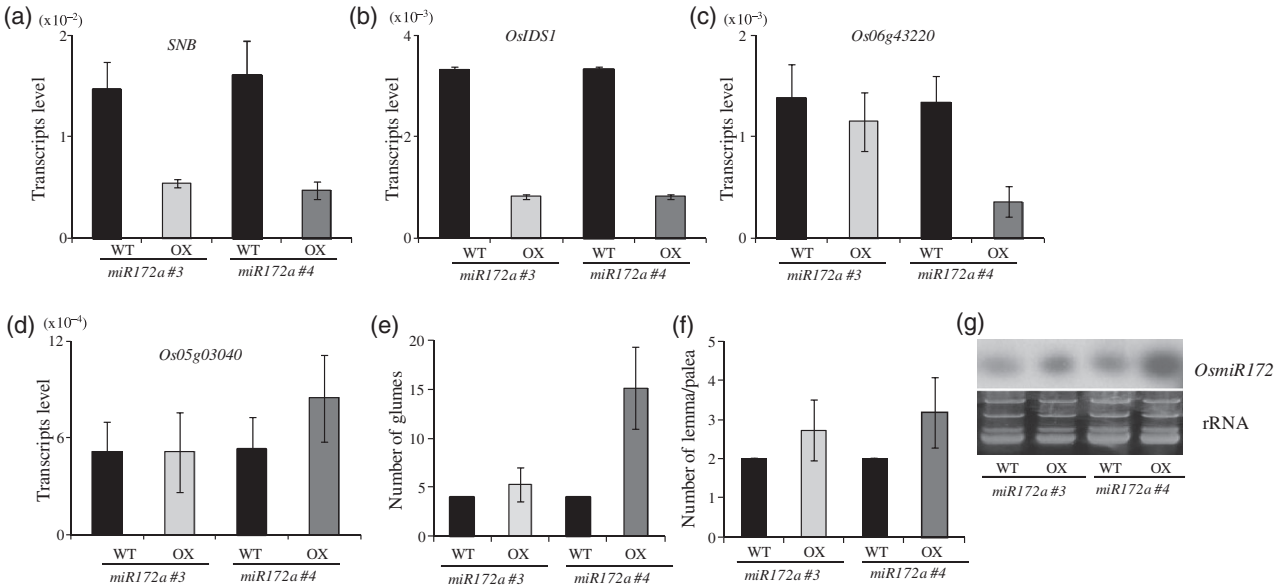

Figure 9. Transcript levels of AP2 family genes in *Ubq::miR172a* inflorescences.
Quantitative RT-PCR analyses were performed in young inflorescences from *Ubq::OsmiR172a* no. 3 and no. 4, and their segregant wild type. Bar represents relative values between transcripts levels of *Ubi1* and AP2 family genes: *SNB* (a), *OsIDS1* (b), *Os06g43220* (c), and *Os05g03040* (d).
Two independent experiments were performed for each overexpressing plant and the wild type. WT and OX are wild-type and overexpressing plants of T_2 siblings. Error bars indicate standard deviation. Inflorescences <10 mm long were used.
(e, f) Summary of phenotypes in *Ubq::OsmiR172a* no. 3 and no. 4 plants. Average number of glumes per spikelet (e). 'Glume' includes rudimentary glume and empty glume. Average numbers of lemma, palea, and lemma/palea-like structures in spikelet (f).
(g) Mature *OsmiR172* levels measured by microRNA northern blot analysis (top). Ethidium bromide-stained ribosomal RNA was used as loading control (bottom).

to the stem–loop RT-PCR analyses, mature *miR172* was highly expressed in leaf sheaths and early-inflorescence meristems (Figure 10b).

To study the spatio-temporal expression pattern, we performed RNA *in situ* hybridization using a DIG-labeled *miR172* antisense LNA probe. Mature *miR172*s were first detected in the branch meristem (Figure 10c), then preferentially expressed in the abaxial regions of that branch meristem, where new spikelet meristems were about to develop (Figure 10f, black arrowhead), and in the half-ring domains of spikelet meristems (Figure 10c,g–i, red arrowheads). The latter trend in expression was similar to that of *FZP* (Figures 5 and 7), whereas *miR172*s were expressed in broader regions. At the later stages of inflorescence development, *miR172*s accumulated throughout the spikelet meristem and recipient spikelet organs (Figure 10d). However, their transcript levels were sharply decreased following transition into a floral meristem (Figure 10e). This preferential expression pattern is consistent with a role for this gene in regulating spikelet development.

DISCUSSION

SNB and *OsIDS1* are required for lodicule identity

Rice possesses a unique floral structure in which the spikelet contains lodicules rather than petals, and lemma and palea instead of sepals. These lodicules are believed to be structurally homologous to petals (Ambrose *et al.*, 2000; Bommert *et al.*, 2005). A lodicule is a small and semitransparent scale that acts to open the palea and lemma for anthesis. Here, single *snb* or *osids1* mutants, as well as their double mutants, showed various phenotypes in the inner floral organs, entailing alterations of lodicule numbers and morphology plus sequential reductions in stamen number. Lodicules from the mutants were frequently elongated into lemma/palea-like structures. In addition, asymmetric distribution of lodicules was disrupted in those mutants, resulting in ectopic lodicules on the palea side. Wild-type rice normally has two lodicules on the lemma side. Therefore, those unnatural lodicules probably developed on the palea side at the expense of stamen formation.

Lodicule identity is specified by B- and E-function genes (Kang *et al.*, 1998; Nagasawa *et al.*, 2003; Cui *et al.*, 2010). Loss of the former class results in abnormal lodicules that enlarge to palea- or glume-like organs (Nagasawa *et al.*, 2003; Prasad and Vijayraghavan, 2003). Likewise, a double knockdown of *OsMADS7* and *OsMADS8*, two E-function genes, leads to homeotic transformation of lodicules into lemma/palea-like organs (Cui *et al.*, 2010). Consistent with this, we observed that lodicule defects in *snb* and *osids1* were accompanied by reduced expression of B-function genes (*OsMADS16*, *OsMADS4*, and *OsMADS2*) and E-function genes (*OsMADS7* and *OsMADS8*). Our *in situ*

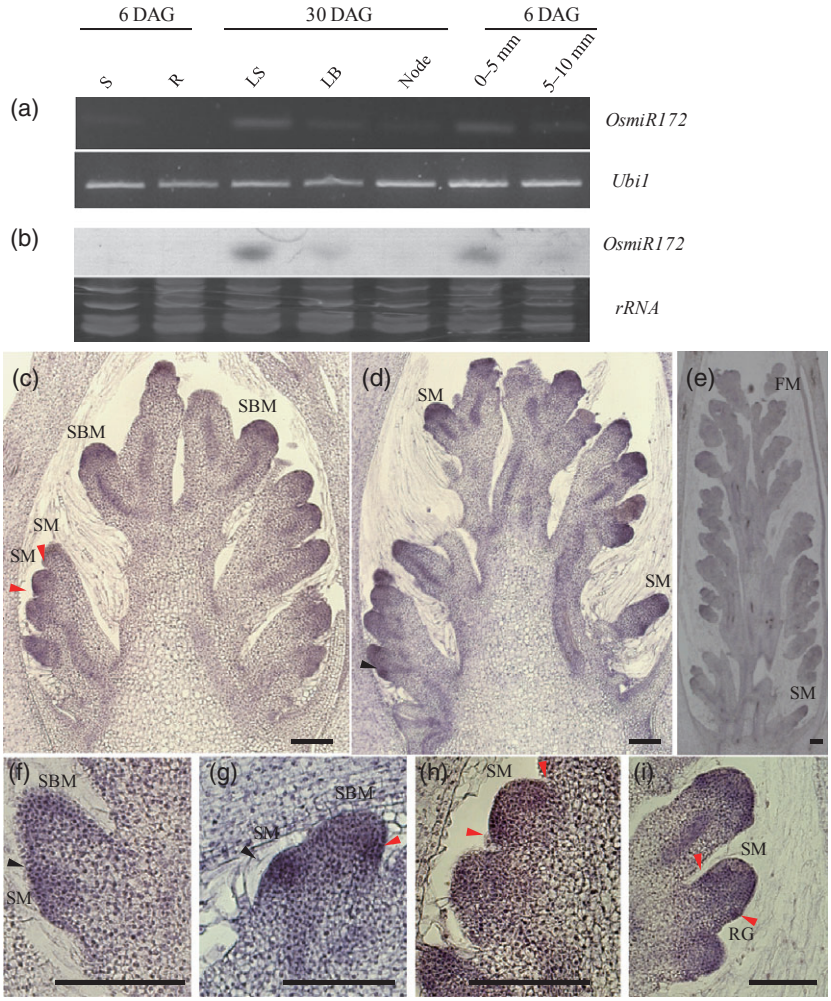

Figure 10. Expression analyses of *OsmiR172*.
(a) Stem–loop RT-PCR analysis in various organs. Rice *Ubi1* served as control.
(b) Gel blot assay of *miR172* levels (upper). Ribosomal RNAs were used as loading controls (lower). DAG, days after germination; IF, inflorescence; LB, leaf blade; LS, leaf sheath; R, roots S, shoots.
(c–e) MicroRNA *in situ* hybridization of *miR172* in early inflorescences. Panicle containing branch meristem and spikelet meristem (c). Panicle with rudimentary glumes emerging from most spikelet meristems (d). Panicle in which most spikelet meristems have produced glumes and lemma/paleas (d). Panicle in which most spikelets have produced floral organs at top position but spikelet meristems still remain at bottom (e).
(f–i) Magnified image of spikelet meristems at stage of their emergence (f), before stage of rudimentary glume primordia emergence (g, h), and after rudimentary glume primordia emerged (i).
Arrowheads indicate *FZP* expression domains. FM; floret meristem; RG, rudimentary glume; SBM, secondary branch meristem; SM, spikelet meristem. Scale bar = 100 μm.

analysis showed that *OsMADS2* and *OsMADS7* transcripts were absent in the elongated lodicules of *snb osids1*. In contrast, *DL* expression was expanded to the reiterated lemma/palea and elongated lodicules in the double mutant (Yamaguchi *et al.*, 2004). All of these observations support, at the molecular level, that the mutations cause an alteration of lodicules to lemma-like organs. Furthermore, we can conclude that *SNB* and *OsIDS1* are required for lodicule development, either by partitioning lodicule-specifying genes or repressing lemma/palea-specifying genes.

Conserved functioning of AP2 family genes in grass spikelet development

The cleistogamous trait, i.e. a self-pollinating habit, arises from a failure in the *miR172*-mediated repression of *cleistogamy1* (*cly1*) in barley (Nair *et al.*, 2010). *CLY1* encodes a two AP2-domain transcription factor related to SNB and OsIDS1 (Figure S1b). Mutation at the *miR172* target site of *CLY1* causes a loss of conductive tissue in the lodicules, so that the lemma and palea fail to open at anthesis (Nair *et al.*, 2010). Similarly, our *snb osids1* spikelets had open hulls due

to this abnormality. Therefore, the role of AP2 family genes in lodicule morphology might be conserved among grass species.

In maize, *ids1* spikelets produce multiple florets instead of the two florets found in the WT (Chuck *et al.*, 1998). Chuck *et al.* (2008) have postulated that ectopic floret formation is caused by increased expression of *SID1* via the liberation of mutual repression between *IDS1* and *SIDS1*. However, we did not observe any such repression between *SNB* and *OsIDS1* (Figure S1d). In our rice, spikelets from *snb* or *osids* single mutants produced extra bract-like structures, but no ectopic florets.

Maize *ids1 sid1* spikelets continuously produce glume-like structures without floral organs (Chuck *et al.*, 2008). Although the rice *snb osids1* spikelets also generated numerous glume-like structures, they eventually produced floral organs. Florets also developed in the *microRNA172*-overexpressing plants. These findings indicated that the rice and maize AP2 genes share some functional similarity, but have unique roles.

Overexpression of *miR172* in Arabidopsis does not affect the mRNA levels of target genes, but it does so at the protein level via translational repression (Aukerman and Sakai, 2003). However, *miR172* can also efficiently guide mRNA cleavage, although the effects on the steady-state level of target transcripts are obscured by strong feedback regulation (Schwab *et al.*, 2005). Similarly, we observed that transcript levels of *SNB* and *OsIDS1* were decreased in the *miR172*-overexpressing rice. However, the extent of these declines was not correlated with the increased level of *miR172* (Figure 9). Moreover, significant amounts of transcript still remained in those lines where *miR172*s were highly accumulated (data not shown). We postulate, therefore, that the action of the rice *miR172* on its target genes is also accomplished by mRNA cleavage or translational repression.

SNB and *OsIDS1* determine rice inflorescence architecture by regulating changes in meristem fate

In rice, panicle architecture is largely controlled by two key factors: (i) the number of primary branches, which is regulated by the timing of inflorescence meristem abortion; and (ii) the number of next-order lateral meristems on each primary branch, which is determined by the timing for conversion of branch meristems into terminal spikelet meristems. In our panicles from *snb osids1*, inflorescence and branch meristems were prematurely converted to next-order meristems, resulting in a decrease in the number of primary branches and spikelets. Thus, one of the roles of *SNB* and *OsIDS1* must be to prevent the precocious determination of inflorescence and branch meristems.

That mutant also showed phenotypes of supernumerary bracts and the homeotic transformation of lodicules into lemma/palea-like organs. We observed that *FZP* expression was increased in its young panicles (Figure 5a). Our RNA *in situ* analysis demonstrated that precocious expression of *FZP* in branch meristems and its continuous expression in spikelet meristems could be attributed to heightened expression in the mutant. Because *FZP* is required for spikelet meristem formation (Komatsu *et al.*, 2003b), these mutant phenotypes were likely due to such extended spikelet fates. Thus, we postulate that the AP2 family genes are repressors of spikelet meristem genes, such as *FZP*, that control spikelet identity during branch meristem ramification.

To investigate their possible interaction, we examined the coincidence of expression between *FZP* and *SNB*. Double RNA *in situ* hybridization indicated that their expressions overlapped in the domain of *FZP* expression, starting at the emergence of spikelet meristems and continuing until they had acquired floral meristem identities. However, *SNB* expression was broader than that of *FZP*, such that their expressions occurred far apart after the rudimentary glumes emerged. Therefore, this *SNB* expression pattern implied that other genes are also regulated by the AP2 gene.

A balance between *miR172* and AP2 family genes determines the ramification of spikelets

Our analyses of mutant phenotypes and marker gene expression suggested that *SNB* and *OsIDS1* are negative regulators of spikelet meristem fate. This hypothesis has now been strengthened by our finding of over-expression for *miR172*, subject to reduced levels of AP2 family genes. Strong *Ubq::miR172* lines had primary branches with only terminal spikelets, and spikelets with more indeterminate bracts. This implies that branch meristems are prematurely determined as spikelets due to the ground level of expression by AP2 family genes.

Because *SNB* and *OsIDS1* are expressed throughout the branch and spikelet meristems, there should be post-transcriptional regulation that reduces the action of AP2 genes in spikelet meristems. When those meristems were initiated here, *miR172* expression was recruited, and subsequently this depleted *SNB* and *OsIDS1* transcripts, ensuring spikelet development at the correct position and time. Therefore, we suggest that *miR172* functions as a major determinant of branch meristem ramification. Similarly, in maize, loss of *zmmiR172e* (*ts4*) and the resistant allele of *ids1* to *miR172* (*ts6*) results in increased branching in spikelet meristems (Chuck *et al.*, 2007). We expected that hampering the AP2 genes by abolishing the microRNA binding affinity would lead to more spikelets per rachis branch. Therefore, we generated transgenic rice plants that over-expressed *miR172*-resistant forms of *SNB* and *OsIDS1*. The transgenic plants showed a phenotype of extremely late flowering, so that no transition to the reproductive phase occurred, even after 1 year. Thus, we were unable to study panicle development in these plants.

In considering the severe phenotypes observed from *miR172*-overexpressing lines, we suspected that another

AP2 gene was involved in the development of branch and spikelet meristems. Our RT-PCR analysis of inflorescences from the *Ubq::miR172* lines suggested that *Os06g43220* probably interacts with *miR172*. Along with their inflorescence characteristics, *miR172*-overexpressing plants showed phenotypes of early flowering and shorter stature, neither of which was observed from *snb osids1*. This implied that other *miR172* target genes are involved in those phenotypes. It will be interesting to study how the vegetative-to-reproductive transition is controlled by these AP2 family genes. Further elucidation of those genes in combination with *SNB* and *OsIDS1* will also lead to a better understanding of plant development.

EXPERIMENTAL PROCEDURES

Plant materials and growth

Mutant lines were isolated from a T-DNA tagging line (*O. sativa* japonica cv. Dongjin and Hwayoung), using our T-DNA flanking sequence database (Jeon *et al.*, 2000; Jeong *et al.*, 2002, 2006; An *et al.*, 2003). Plants were reared in an isolated rice paddy field, a greenhouse supplied with artificial light, or growth rooms under short-day (SD; 10-h light) or long-day (LD; 14-h light) conditions.

RNA isolation and RT-PCR analysis

Total RNA was extracted using RNA iso (Takara Bio Inc., http://www.takara-bio.com/). The residual DNA in each RNA sample was removed by RQ1 RNase-Free DNase (Promega, http://www.promega.com/). Complementary DNA was synthesized as previously reported (Han *et al.*, 2006). The primers were as follows: for *SNB*, 5′-ATGGAAGGGAAGCTGTTACT-3′ and 5′-AATGTGGATG CTGGGACATC-3′; for *OsIDS1*, 5′-AAGGAGGAGTTCGTGCACAT-3′ and 5′-GGCGCCGGCAGAGAATCCT-3′; and for *Ubi1*, 5′-AACCAA GATCGGCAGTATGG-3′ and 5′-GATTGATTGCTCCAGCAGGC-3′.

Quantitative real-time RT-PCR

Rice cDNA was prepared from young panicles. Real-time PCR was performed with a Rotor-Gene® 6000 light cycler (Corbett Life Science, http://www.corbettlifescience.com/) as described by Han *et al.* (2006). The primers are represented in Table S1.

RNA *in situ* hybridization

The RNA *in situ* hybridization was performed as described by Lee *et al.* (2007). For probe generation, the PCR primers were: for *OsIDS1*, 5′-ACTCGATCGAAGTCGGAAGA-3′ and 5′-GCGACCACC GGCCGCT-3′; *FZP*, 5′-GTCATGAACACTCGAGGC-3′ and 5′-CAGAGG CAAAGTGCGTGAT-3′; *OsMADS7*, 5′-GAGCAGGGCTGCAACTT AAT-3′ and 5′-CGCTTAAAGTTGATCGCAGA-3′; *OsMADS2*, 5′-GAAG ACGAGAACAAGCTGCT-3′ and 5′-TTCAATCCAGTGGTGGATCA-3′; and *DL*, 5′-AATGGATCTCGTGTCGCCGT-3′ and 5′-GAGGCGGTG TTTCTTCTCTG-3′.

For double RNA *in situ* hybridization, the *SNB* and *FZP* probes were labeled with DIG and fluorescein, respectively. Both probes were placed on the same slides during hybridization. For detection, anti-DIG-AP and anti-fluorescein-AP (Roche, http://www.roche.com/) were incubated at 1:1000 and 1:10 000 dilutions, respectively. After nitro-blue tetrazolium/5-bromo-4-chloro-3′-indolyphosphate (NBT/BCIP) substrates were used for visualizing the SNB-DIG probe, the slides were incubated in 0.1 M glycine–HCl (pH 2.2) for 20 min to inactivate the alkaline phosphatase. Afterward, 2-(4-iodophenyl)-5-(4-nitrophenyl)-3-phenyltetrazolium (INT/BCIP) substrates (Roche) were used sequentially for the FZP-fluorescein probe. Images were photographed from a BX61 microscope (Olympus, http://www.olympus.com/).

Generation of *microRNA172*-overexpressing plants

The *miR172* spanning regions were isolated from genomic DNA by PCR, using OsmiR172a oligos (5′-ACGGTAGAGTCGGTGTTTGC-3′, 5′-CATTGTGAAACGGAGGGAGT-3′), OsmiR172b oligos (5′-ACAGA AAGAGGGAGGGAGGA-3′, 5′-TGTAGCTGCATGCTAGGTAG-3′), miR172c oligos (5′-GCACGTAGACAACCATGCAC-3′, 5′-CACAGCCC GTTCGTTGTAG-3′), and miR172d oligos (5′-CATGGATCGAGACGA GTAG-3′, 5′-TGCATATATGGAGCTAGTAG-3′). The PCR fragment was cloned into the pGA1611 binary vector (Kim *et al.*, 2009) and the construct was transformed into *Agrobacterium tumefaciens* LBA4404 (An *et al.*, 1988). The procedure for transforming rice via *Agrobacterium*-mediated co-cultivation was described previously (Jeon *et al.*, 1999).

Expression analyses of microRNA

Pulsed reverse-transcription reactions and PCR were performed as described by Varkonyi-Gasic *et al.* (2007). Reactions included 200 units of Moloney murine leukemia virus (M-MLV) reverse transcriptase (Promega), purified total RNA, 0.25 mM dNTPs, and 50 nM miR172 RT primer (5′-GTTGGCTCTGGTGCAGGGTCCGAGGT ATTCGCACCAGAGCCAACATGCAG-3′), which binds to the 3′ portion of microRNA. The reaction was started at 16°C for 30 min, followed by pulsed reverse-transcription for 60 cycles at 30°C for 30 sec, 42°C for 30 sec, and 50°C for 1 sec. The reaction was then terminated by incubating at 85°C for 5 min. Products were PCR-amplified with an miRNA172 forward primer (5′-GCGGCGAGAAT CTTGATGATG-3′) and a universal primer (5′-TGCAGGGTCCGA GGT-3′). The reaction included an initial 2-min denaturation at 94°C, followed by 20 to 40 cycles of 94°C for 15 sec and 60°C for 1 min. RNA gel blot analysis was performed using 2 μg of total RNA and a P^{32}-labeled antisense oligonucleotide probe (miR172LNA AS, 5′-ATgCAgCAtCAtCAaGAtTCT-3′; upper- and lower-case letters indicate DNA and LNA, respectively) (Varallyay *et al.*, 2008). For microRNA *in situ* hybridization, the antisense LNA oligonucleotide was 3′ end-labeled with DIG-ddUTP by terminal transferase (Roche, http://www.roche.com/). Beforehand, tissue sections were treated with 0.16 M 1-ethyl-3-(dimethyl aminopropyl) carbomide (EDC) solutions for 2 h to prevent the loss of microRNA (Pena *et al.*, 2009). Hybridization was then conducted at 37°C.

ACKNOWLEDGEMENTS

We thank Kyungsook An for generating the transgenic lines and managing the transgenic seeds, and Priscilla Licht for English editing of the manuscript. This work was supported in part by grants from the Next-Generation BioGreen 21 Program (Plant Molecular Breeding Center, No. PJ008128), Rural Development Administration, Republic of Korea; the Basic Research Promotion Fund, Republic of Korea (KRF-2007-341-C00028); from the Technology Development Program for Agriculture and Forestry, Ministry for Food, Agriculture, Forestry and Fisheries, Republic of Korea (309017-5); and Kyung Hee University (20110269).

SUPPORTING INFORMATION

Additional Supporting Information may be found in the online version of this article:

Figure S1. Molecular analyses of *OsIDS1* and *SNB*.

Figure S2. Scanning electron microscope image of wild-type and *snb osids1* spikelets.

Figure S3. Spikelet phenotypes of *snb osids1*.
Figure S4. Phenotype variations under short and long days.
Figure S5. Messenger RNA levels of *SNB* and *OsIDS1* in inflorescences of *snb osids1.*
Table S1. List of primers used in the quantitative RT-PCR.
As a service to our authors and readers, this journal provides supporting information supplied by the authors. Such materials are peer-reviewed and may be re-organized for online delivery, but are not copy-edited or typeset. Technical support issues arising from supporting information (other than missing files) should be addressed to the authors.

REFERENCES

Ambrose, B.A., Lerner, D.R., Ciceri, P., Padilla, C.M., Yanofsky, M.F. and Schmidt, R.J. (2000) Molecular and genetic analyses of the silky1 gene reveal conservation in floral organ specification between eudicots and monocots. *Mol. Cell*, **5**, 569–579.

An, G., Ebert, P.R., Mitra, A. and Ha, S.B. (1988) Binary vectors. In *Plant Molecular Biology Manual* (Gelvin, S.B. and Schilperoort, R.A., eds). Dordrecht, The Netherlands: Kluwer Academic Publishers, pp 1–19.

An, S., Park, S., Jeong, D.H. *et al.* (2003) Generation and analysis of end sequence database for T-DNA tagging lines in rice. *Plant Physiol.* **133**, 2040–2047.

Arber, A.R. (1934) *The Gramineae: A Study of Cereal, Bamboo, and Grass*. Cambridge, UK: Cambridge Univ Press.

Ashikari, M., Sakakibara, H., Lin, S. *et al.* (2005) Cytokinin oxidase regulates rice grain production. *Science*, **309**, 741–745.

Aukerman, M.J. and Sakai, H. (2003) Regulation of flowering time and floral organ identity by a MicroRNA and its APETALA2-like target genes. *Plant Cell*, **15**, 2730–2741.

Bommert, P., Satoh-Nagasawa, N., Jackson, D. and Hirano, H.Y. (2005) Genetics and evolution of inflorescence and flower development in grasses. *Plant Cell Physiol.* **46**, 69–78.

Bortiri, E. and Hake, S. (2007) Flowering and determinacy in maize. *J. Exp. Bot.* **58**, 909–916.

Chen, X. (2004) A microRNA as a translational repressor of APETALA2 in *Arabidopsis* flower development. *Science*, **303**, 2022–2025.

Chen, C., Ridzon, D.A., Broomer, A.J. *et al.* (2005) Real-time quantification of microRNAs by stem-loop RT-PCR. *Nucleic Acids Res.* **33**, e179.

Chuck, G., Meeley, R.B. and Hake, S. (1998) The control of maize spikelet meristem fate by the APETALA2-like gene indeterminate spikelet1. *Genes Dev.* **12**, 1145–1154.

Chuck, G., Muszynski, M., Kellogg, E., Hake, S. and Schmidt, R.J. (2002) The control of spikelet meristem identity by the branched silkless1 gene in maize. *Science*, **298**, 1238–1241.

Chuck, G., Meeley, R., Irish, E., Sakai, H. and Hake, S. (2007) The maize tasselseed4 microRNA controls sex determination and meristem cell fate by targeting Tasselseed6/indeterminate spikelet1. *Nat. Genet.* **39**, 1517–1521.

Chuck, G., Meeley, R. and Hake, S. (2008) Floral meristem initiation and meristem cell fate are regulated by the maize AP2 genes ids1 and sid1. *Development*, **135**, 3013–3019.

Chung, Y.Y., Kim, S.R., Finkel, D., Yanofsky, M.F. and An, G. (1994) Early flowering and reduced apical dominance result from ectopic expression of a rice MADS box gene. *Plant Mol. Biol.* **26**, 657–665.

Cui, R., Han, J., Zhao, S., Su, K., Wu, F., Du, X., Xu, Q., Chong, K., Theissen, G. and Meng, Z. (2010) Functional conservation and diversification of class E floral homeotic genes in rice (*Oryza sativa*). *Plant J.* **61**, 767–781.

Fornara, F., Parenicova, L., Falasca, G., Pelucchi, N., Masiero, S., Ciannamea, S., Lopez-Dee, Z., Altamura, M.M., Colombo, L. and Kater, M.M. (2004) Functional characterization of OsMADS18, a member of the AP1/SQUA subfamily of MADS box genes. *Plant Physiol.* **135**, 2207–2219.

Greco, R., Stagi, L., Colombo, L., Angenent, G.C., Sari-Gorla, M. and Pe, M.E. (1997) MADS box genes expressed in developing inflorescences of rice and sorghum. *Mol. Gen. Genet.* **253**, 615–623.

Han, M.J., Jung, K.H., Yi, G., Lee, D.Y. and An, G. (2006) Rice Immature Pollen 1 (RIP1) is a regulator of late pollen development. *Plant Cell Physiol.* **47**, 1457–1472.

Honma, T. and Goto, K. (2001) Complexes of MADS-box proteins are sufficient to convert leaves into floral organs. *Nature*, **409**, 525–529.

Hoshikawa, K. (1989) *The Growing Rice Plant*. Tokyo: Nobunkyo.

Huang, X., Qian, Q., Liu, Z., Sun, H., He, S., Luo, D., Xia, G., Chu, C., Li, J. and Fu, X. (2009) Natural variation at the DEP1 locus enhances grain yield in rice. *Nat. Genet.* **41**, 494–497.

Ikeda, K., Sunohara, I. and Nagato, Y. (2004) Developmental course of inflorescence and spikelet in rice. *Breed. Sci.* **54**, 147–156

Ikeda, K., Ito, M., Nagasawa, N., Kyozuka, J. and Nagato, Y. (2007) Rice ABERRANT PANICLE ORGANIZATION 1, encoding an F-box protein, regulates meristem fate. *Plant J.* **51**, 1030–1040.

Ikeda-Kawakatsu, K., Yasuno, N., Oikawa, T., Iida, S., Nagato, Y., Maekawa, M. and Kyozuka, J. (2009) Expression level of ABERRANT PANICLE ORGANIZATION1 determines rice inflorescence form through control of cell proliferation in the meristem. *Plant Physiol.* **150**, 736–747.

Itoh, J., Nonomura, K., Ikeda, K., Yamaki, S., Inukai, Y., Yamagishi, H., Kitano, H. and Nagato, Y. (2005) Rice plant development: from zygote to spikelet. *Plant Cell Physiol.* **46**, 23–47.

Jeon, J.S., Chung, Y.Y., Lee, S., Yi, G.H., Oh, B.G. and An, G. (1999) Isolation and characterization of an anther-specific gene, RA8, from rice (*Oryza sativa* L.). *Plant Mol. Biol.* **39**, 35–44.

Jeon, J.-S., Lee, S., Jung, K.-H., Yang, W.-S. and An, G. (2000) Production of transgenic rice plants showing reduced heading date and plant height by ectopic expression of rice MADS-box genes. *Mol. Breed.* **6**, 581–592.

Jeon, J.S., Lee, S. and An, G. (2008) Intragenic control of expression of a rice MADS box gene OsMADS1. *Mol. Cells*, **26**, 474–480.

Jeong, D.H., An, S., Kang, H.G., Moon, S., Han, J.J., Park, S., Lee, H.S., An, K. and An, G. (2002) T-DNA insertional mutagenesis for activation tagging in rice. *Plant Physiol.* **130**, 1636–1644.

Jeong, D.H., An, S., Park, S. *et al.* (2006) Generation of a flanking sequence-tag database for activation-tagging lines in japonica rice. *Plant J.* **45**, 123–132.

Kang, H.G., Jeon, J.S., Lee, S. and An, G. (1998) Identification of class B and class C floral organ identity genes from rice plants. *Plant Mol. Biol.* **38**, 1021–1029.

Kellogg, E.A. (2007) Floral displays: genetic control of grass inflorescences. *Curr. Opin. Plant Biol.* **10**, 26–31.

Kim, S.R., Lee, D.Y., Yang, J.I., Moon, S. and An, G. (2009) Cloning vectors for rice. *J. Plant Biol.* **52**, 73–78.

Kobayashi, K., Maekawa, M., Miyao, A., Hirochika, H. and Kyozuka, J. (2010) PANICLE PHYTOMER2 (PAP2), encoding a SEPALLATA subfamily MADS-box protein, positively controls spikelet meristem identity in rice. *Plant Cell Physiol.* **51**, 47–57.

Komatsu, K., Maekawa, M., Ujiie, S., Satake, Y., Furutani, I., Okamoto, H., Shimamoto, K. and Kyozuka, J. (2003a) LAX and SPA: major regulators of shoot branching in rice. *Proc. Natl Acad. Sci. USA*, **100**, 11765–11770.

Komatsu, M., Chujo, A., Nagato, Y., Shimamoto, K. and Kyozuka, J. (2003b) FRIZZY PANICLE is required to prevent the formation of axillary meristems and to establish floral meristem identity in rice spikelets. *Development*, **130**, 3841–3850.

Kumar, R., Singh, S.K., Koshkin, A.A., Rajwanshi, V.K., Meldgaard, M. and Wengel, J. (1998) The first analogues of LNA (locked nucleic acids): phosphorothioate-LNA and 2′-thio-LNA. *Bioorg. Med. Chem. Lett.* **8**, 2219–2222.

Kyozuka, J., Kobayashi, T., Morita, M. and Shimamoto, K. (2000) Spatially and temporally regulated expression of rice MADS box genes with similarity to *Arabidopsis* class A, B and C genes. *Plant Cell Physiol.* **41**, 710–718.

Lauter, N., Kampani, A., Carlson, S., Goebel, M. and Moose, S.P. (2005) microRNA172 down-regulates glossy15 to promote vegetative phase change in maize. *Proc. Natl Acad. Sci. USA*, **102**, 9412–9417.

Lee, D.Y., Lee, J., Moon, S., Park, S.Y. and An, G. (2007) The rice heterochronic gene SUPERNUMERARY BRACT regulates the transition from spikelet meristem to floral meristem. *Plant J.* **49**, 64–78.

Nagasawa, N., Miyoshi, M., Sano, Y., Satoh, H., Hirano, H., Sakai, H. and Nagato, Y. (2003) SUPERWOMAN1 and DROOPING LEAF genes control floral organ identity in rice. *Development*, **130**, 705–718.

Nair, S.K., Wang, N., Turuspekov, Y. *et al.* (2010) Cleistogamous flowering in barley arises from the suppression of microRNA-guided HvAP2 mRNA cleavage. *Proc. Natl Acad. Sci. USA*, **107**, 490–495.

Nakagawa, M., Shimamoto, K. and Kyozuka, J. (2002) Overexpression of RCN1 and RCN2, rice TERMINAL FLOWER 1/CENTRORADIALIS homologs, confers delay of phase transition and altered panicle morphology in rice. *Plant J.* **29**, 743–750.

Pelaz, S., Ditta, G.S., Baumann, E., Wisman, E. and Yanofsky, M.F. (2000) B and C floral organ identity functions require SEPALLATA MADS-box genes. *Nature*, **405**, 200–203.

Pelucchi, N., Fornara, F., Favalli, C., Masiero, S., Lago, C., Pè, M.E., Colombo, L. and Kater, M.M. (2002) Comparative analysis of rice MADS-box genes expressed during flower development. *Sex. Plant Reprod.* **15**, 113–122.

Pena, J.T., Sohn-Lee, C., Rouhanifard, S.H. *et al.* (2009) miRNA in situ hybridization in formaldehyde and EDC-fixed tissues. *Nat. Methods*, **6**, 139–141.

Prasad, K. and Vijayraghavan, U. (2003) Double-stranded RNA interference of a rice PI/GLO paralog, OsMADS2, uncovers its second-whorl-specific function in floral organ patterning. *Genetics*, **165**, 2301–2305.

Prasad, K., Sriram, P., Kumar, C.S., Kushalappa, K. and Vijayraghavan, U. (2001) Ectopic expression of rice OsMADS1 reveals a role in specifying the lemma and palea, grass floral organs analogous to sepals. *Dev. Genes. Evol.* **211**, 281–290.

Rao, N.N., Prasad, K., Kumar, P.R. and Vijayraghavan, U. (2008) Distinct regulatory role for RFL, the rice LFY homolog, in determining flowering time and plant architecture. *Proc. Natl Acad. Sci. USA*, **105**, 3646–3651.

Schmid, M., Uhlenhaut, N.H., Godard, F., Demar, M., Bressan, R., Weigel, D. and Lohmann, J.U. (2003) Dissection of floral induction pathways using global expression analysis. *Development*, **130**, 6001–6012.

Schmidt, R.J. and Ambrose, B.A. (1998) The blooming of grass flower development. *Curr. Opin. Plant Biol.* **1**, 60–67.

Schwab, R., Palatnik, J.F., Riester, M., Schommer, C., Schmid, M. and Weigel, D. (2005) Specific effects of microRNAs on the plant transcriptome. *Dev. Cell*, **8**, 517–527.

Sunkar, R., Girke, T., Jain, P.K. and Zhu, J.K. (2005) Cloning and characterization of microRNAs from rice. *Plant Cell*, **17**, 1397–1411.

Varallyay, E., Burgyan, J. and Havelda, Z. (2008) MicroRNA detection by northern blotting using locked nucleic acid probes. *Nat. Protoc.* **3**, 190–196.

Varkonyi-Gasic, E., Wu, R., Wood, M., Walton, E.F. and Hellens, R.P. (2007) Protocol: a highly sensitive RT-PCR method for detection and quantification of microRNAs. *Plant Methods*, **3**, 12.

Weigel, D., Alvarez, J., Smyth, D.R., Yanofsky, M.F. and Meyerowitz, E.M. (1992) LEAFY controls floral meristem identity in *Arabidopsis*. *Cell*, **69**, 843–859.

Yamaguchi, T., Nagasawa, N., Kawasaki, S., Matsuoka, M., Nagato, Y. and Hirano, H.Y. (2004) The YABBY gene DROOPING LEAF regulates carpel specification and midrib development in *Oryza sativa*. *Plant Cell*, **16**, 500–509.

Zhu, Q.H., Upadhyaya, N.M., Gubler, F. and Helliwell, C.A. (2009) Over-expression of miR172 causes loss of spikelet determinacy and floral organ abnormalities in rice (*Oryza sativa*). *BMC Plant Biol.* **9**, 149.

